

# ZERO-SHOT BIAS CORRECTION: EFFICIENT MR IMAGE INHOMOGENEITY REDUCTION WITHOUT ANY DATA

Hongxu Yang<sup>\*</sup>, Edina Timko<sup>\*</sup>, Brice Fernandez<sup>†</sup>

<sup>\*</sup>STO-Artificial Intelligence & Machine Learning, GE HealthCare

<sup>†</sup> IMG-MR-Applications & Workflow, GE HealthCare

## ABSTRACT

In recent years, deep neural networks for image inhomogeneity reduction have shown promising results. However, current methods with (un)supervised solutions require preparing a training dataset, which is expensive and laborious for data collection. In this work, we demonstrate a novel zero-shot deep neural networks, which requires no data for pre-training and dedicated assumption of the bias field. The designed light-weight CNN enables an efficient zero-shot adaptation for bias-corrupted image correction. Our method provides a novel solution to mitigate the biased corrupted image as iterative homogeneity refinement, which therefore ensures the considered issue can be solved easier with stable convergence of zero-shot optimization. Extensive comparison on different datasets show that the proposed method performs better than current data-free N4 methods in both efficiency and accuracy.

**Index Terms**— MRI, inhomogeneity reduction, zero-shot learning

## 1. INTRODUCTION

Magnetic Resonance Imaging (MRI) provides detailed anatomy information of patient, which are essential for accurate and precise diagnosis and analysis. Nevertheless, MRI images are commonly degraded by several different artifacts, which hampers the information in the obtained data. Image inhomogeneity in MRI, which is commonly caused by bias field from imperfect scanner (such as phased-array coils) and magnetic field distribution. With this scanning phenomenon in MRI, the signal intensity within the same anatomy would have a larger low-frequency variance across the obtained volume. Although this inhomogeneity might not be impacting the diagnoses by experienced clinicians, it would drastically degrade the subsequent image processing algorithms and methods, such as registration and segmentation in the fully automated image pipeline. Inhomogeneity removal in MRI has been studied during past decades, and the approaches are categorized as prospective and retrospective methods [1]. The prospective methods are commonly correcting the bias

in the scanning step, which requires dedicated hardware and software design, and therefore economically expensive for medical device companies. In contrast, retrospective methods are processing the obtained images by various image processing techniques to reduce the inhomogeneity and bias in the data. The commonly considered correction methods can be classified into non-learning-based method and learning-based method. Specifically, the most popular non-learning-based method of bias correction is the nonparametric nonuniformity intensity normalization (N3) method [2], and also its modification N4 [3]. Although these methods mostly achieved promising performances and widely accepted by communities of MR imaging, iteration computing on histogram and frequency correction has made these methods time consuming [4]. In addition, as shown in the literature, the N4 method tends to produce unrealistic results when the variance of the bias values are too large [5]. Recent years, (deep) learning-based correction have received remarkable attention in different artifacts reduction application. Supervised deep learning methods were developed for bias-free MRI generation with great success [6, 7]. However, as known in the community, supervised learning methods are suffering lack of large amount of training images with ground truth. To tackle this limitation, unsupervised inhomogeneity correction methods with deep learning (DL) strategies were proposed, such as implicitly trained CNN [8] and histogram-based entropy correction method [4]. The aforementioned methods achieved comparable performances w.r.t. commonly applied N4 algorithm while reducing the annotation efforts of ground truth generation. Nevertheless, there are still several considerations about these methods. First, the implicitly trained CNN requires proper bias field simulation of the images, which is highly correlated to devices and anatomies. Therefore, dedicated research and training data preparation is inevitable. Second, to train a model that can be generalized to different situation, laborious data collection is needed and can be expensive for data preparations. Third, the network trained on such dataset suffers performance drop if the testing datasets are derived from different data distributions. All the above concerns motivated us to study the data-free method.

This paper presents a zero-shot inhomogeneity correction method based on deep learning. The method, as will be ex-



point. With high-order estimation of the HC, the pixel-based regional corruption can be adaptive refined, which is specifically defined as (without considering voxel position)

$$HC^n = HC^{n-1} + \alpha HC^{n-1}(1 - HC^{n-1}) \quad (3)$$

where parameter  $n$  is the number of iteration, which controls the strength of the homogeneity correction and was chosen to be 4 in the paper to trade-off accuracy and computation cost [9].

The above correction would lead to the overestimation for correcting the bias corruption. To constrain the predicted  $\hat{X}$  without over-exposure, the image prior loss is considered. Conventional bias correction methods directly predict the bias field  $B$  with proper constraint [8]. In contrast, without knowing the actual bias of the image, the predicted  $\hat{B}$  in the proposed model is constrained by the image prior, i.e., minimizing  $|Y - \hat{X}\hat{B}|$ , which therefore ensures the homogeneity refined image with predicted bias field can match the input.

## 2.2. CNN Model Design

The CNN model with skip-connection design is depicted in Fig. 1. The 3D volumetric MRI image is downsampled by factor of 8 before processed by Depthwise Separable Convolutions (DSC), which consists of 3D depthwise convolution with kernel size 3 and 3D pointwise convolution with kernels size 1. The purpose of these light-weight design is to reduce the online optimization cost for a standard 3D volumetric data, and accelerate the optimization. With two predicted parametric maps from the last layer (which are interpolated to original resolution), the input data with original resolution is operated by two nonparametrical modules for inhomogeneity and image prior constraint. In our design, the parametric map  $\alpha$  is normalized by Tanh function, while the predicted bias map is multiplied with the predicted images to match input, normalized by Sigmoid.

## 2.3. Online Optimization

The proposed zero-shot model performs the online optimization at testing phase. To properly constraint the model to correct bias field, the designed objective function consists of two parts for joint training.

$$L(\theta) = L_{hc}(\theta) + L_{prior}(\theta) \quad (4)$$

Function  $L_{hc}(\theta)$  is designed to optimize the homogeneity correction function (HC) for CNN with parameters  $\theta$ . Specifically, this function consists of several components as below.

$$L_{hc}(\theta) = L_{smo}(\alpha) + L_{spa}(HC^n, Y) + L_{exp}(HC^n) \quad (5)$$

where  $L_{smo}$  is the smoothness function, which is defined as

$$L_{smo}(\alpha) = \frac{1}{N} \sum_{n=1}^N \left( \sum_{k \in \{x,y,z\}} |\nabla_k \alpha_n| \right)^2 \quad (6)$$

Loss spatial consistency loss  $L_{spa}$  is defined as

$$L_{spa}(HC^n, Y) = \frac{1}{K} \sum_{n=1}^K \sum_{j \in \Omega(i)} (|\hat{HC}_i^n - \hat{HC}_j^n| - |\hat{Y}_i - \hat{Y}_j|)^2 \quad (7)$$

where  $K$  is the number of local region, and  $\Omega(i)$  is the 8 neighboring voxels. The symbol  $\hat{*}$  denotes the average intensity value of the local volume in the image. The  $L_{exp}$  is the exposure loss function to constrain the average regional values of the predicted images [9]. The weights of smoothing loss are empirically selected as 1600 for  $L_{hc}$ , as suggested by Zero-DCE++ [9].

Function  $L_{prior}(\theta)$  is designed to constrain the predicted  $\hat{X}\hat{B}$  to match  $Y$ . Specifically, this loss function is formulated as

$$L_{prior} = |Y - \hat{X}\hat{B}|_1 + L_{smo}(\hat{B}) \quad (8)$$

## 3. EXPERIMENTS AND RESULTS

### 3.1. Dataset

The proposed zero-shot bias correction method was evaluated on five different MRI datasets. First, we randomly selected 39 3D Sagittal T1w MRI brain images from ADNI dataset [10], which are processed by ANTsPyNet [11] to obtain mask of grey matter (GW) white matter (WM), and cerebrospinal fluid (CSF). Second, 59 T1w MR brain images were randomly selected from IXI dataset<sup>1</sup>, which were processed to have anatomy masks same as ADNI dataset. Third, 21 T2w MR brain images were randomly selected from OASIS3 dataset [12], the anatomy masks for GW, MW and CSF were also generated for evaluation. In addition, a private Dixon (DX) dataset with 7 patients was considered, which have water sequences (W) and fat sequences (F) for pelvis region. The sequences were segmented to have bladder (BLD), water and fat components for evaluation purposes. All the used datasets were approved by the ethical committee for research purpose.

### 3.2. Experiment settings

During the execution stage, the designed zero-shot model is optimized by standard Adam optimizer with learning rate equals to 0.005 for ADNI/IXI/OASIS datasets, and 0.0005 for DX datasets, with weight decay equals to 0.0001. The total iteration step is selected to be 100 to balance the efficiency and accuracy.

The evaluation metric was the Coefficient of Variation (CV) for all the considered datasets via the aforementioned anatomy masks. We compared the proposed method to the state-of-the-art N4 method, which is implemented in ANTs toolbox via ITK implementation [11].

<sup>1</sup><https://brain-development.org/ixi-dataset/>

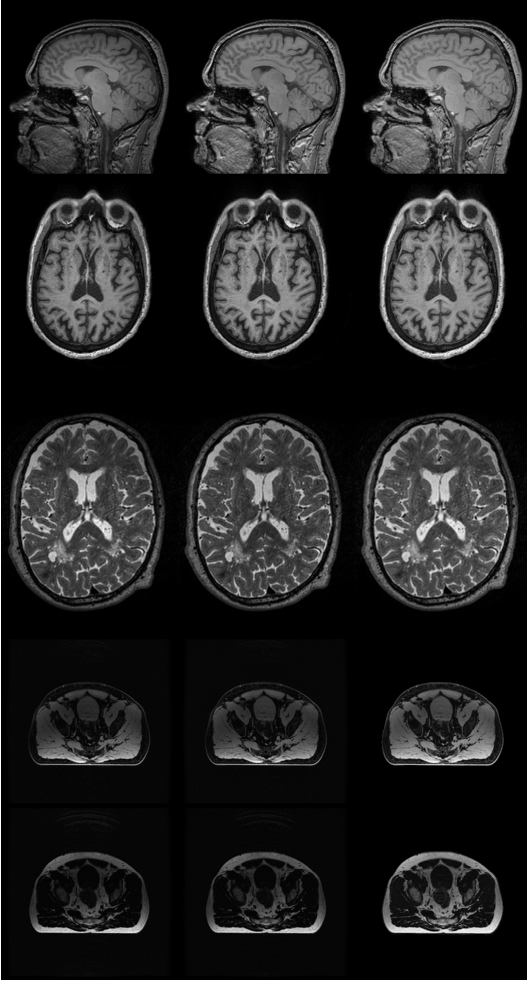


**Fig. 2.** Example images of comparisons. From top to bottom: IXI, ADNI, OASIS, Dixon-water and Dixon-fat. First column: original image, second column: N4 result, third column: the results of the zero-shot bias correction.

### 3.3. Experiment results

The numerical performances are summarized in Table. 1. As can be observed, the zero-shot bias correction achieved better numerical values in Dixon dataset for both bladder and water(fat) regions. As for T1w brain images from different dataset, the proposed method achieved comparable performance to N4 algorithm on white matters, but better performance on grey matters and CSF. Example images from considered datasets are shown in Fig. 2. From the image, N4 method will fail in challenging Dixon images, while our method can better correct the inhomogeneities.

The average execution time of the proposed method on an NVIDIA-A100 is 3 sec., while it can be degraded to around half minute on NVIDIA-P6000 for the considered ADNI dataset. In contrast, N4 method is measured on a CPU of AMD EPYC 7742 with around 800 sec. on ADNI dataset.

**Table 1.** Evaluation results of the method on different dataset, measured by CV with mean(std.)

Dataset	Tissue	Original	N4	Proposed
ADNI	GM	0.194(0.022)	0.163(0.027)	0.149(0.019)
	WM	0.155(0.017)	0.118(0.020)	0.104(0.014)
	CSF	0.564(0.065)	0.558(0.067)	0.492(0.062)
IXI	GM	0.150(0.031)	0.120(0.013)	0.117(0.013)
	WM	0.126(0.027)	0.084(0.007)	0.085(0.011)
	CSF	0.586(0.075)	0.565(0.065)	0.519(0.057)
OASIS	GM	0.356(0.059)	0.338(0.064)	0.304(0.057)
	WM	0.248(0.060)	0.234(0.064)	0.216(0.053)
	CSF	0.694(0.083)	0.659(0.080)	0.619(0.070)
DX-W	BLD	0.159(0.036)	0.138(0.028)	0.118(0.029)
	Water	0.498(0.038)	0.464(0.054)	0.262(0.031)
DX-F	BLD	0.524(0.128)	0.521(0.130)	0.469(0.109)
	Fat	0.521(0.025)	0.505(0.022)	0.273(0.064)

With state-of-the-art deep learning based automated pipelines with a dedicated GPU, the proposed method shows faster processing time than the commonly used N4 algorithm, but much better results on challenging strong bias field MRIs.

## 4. CONCLUSIONS

This paper presents a novel zero-shot data-free deep learning solution for inhomogeneity correction for MR 3D volumetric data. This novel approach introduces an alternative view-points of solving the bias corrupted images, which showed its better ability to achieve better performance than the current solutions. With dedicated evaluation on different MR sequences, the propose achieved comparable or even better numerical results than popular N4 bias correction method, while significantly accelerating the operating speed to just seconds. Therefore, the full automated MRI pipelines, such as end-to-end automated Alzheimer’s disease analysis, can be drastically accelerated for pre-processing steps.

## 5. ACKNOWLEDGEMENT

PREDICTOM receives funding from the Innovative Health Initiative Joint Undertaking (IHI JU), under Grant Agreement No 101132356. JU receives support from the European Union’s Horizon Europe research and innovation programme, COCIR, EFPIA, EuropaBio, MedTechEurope and Vaccines Europe. The UK participants are supported by UKRI Grant No 10083467 (National Institute for Health and Care Excellence), Grant No 10083181 (King’s College London), and Grant No 10091560 (University of Exeter). The Swiss participant is supported by the Swiss State Secretariat for Education, Research and Innovation Ref No 113152304. See <https://www.predictom.eu/> for more details

## 6. REFERENCES

- [1] Uro Vovk, Franjo Pernus, and Botjan Likar, "A review of methods for correction of intensity inhomogeneity in mri," *IEEE transactions on medical imaging*, vol. 26, no. 3, pp. 405–421, 2007.
- [2] John G Sled, Alex P Zijdenbos, and Alan C Evans, "A nonparametric method for automatic correction of intensity nonuniformity in mri data," *IEEE transactions on medical imaging*, vol. 17, no. 1, pp. 87–97, 1998.
- [3] Nicholas J Tustison, Brian B Avants, Philip A Cook, Yuanjie Zheng, Alexander Egan, Paul A Yushkevich, and James C Gee, "N4itk: improved n3 bias correction," *IEEE transactions on medical imaging*, vol. 29, no. 6, pp. 1310–1320, 2010.
- [4] Maria Perez-Caballero, Sergio Morell-Ortega, Marina Ruiz Perez, Pierrick Coupe, and Jose V Manjon, "Unsupervised deep learning method for bias correction," in *Medical Imaging with Deep Learning*, 2024.
- [5] Dong Liang, Xingyu Qiu, Kuanquan Wang, Gongning Luo, Wei Wang, and Yashu Liu, "Unsupervised decomposition networks for bias field correction in mr image," *arXiv preprint arXiv:2307.16219*, 2023.
- [6] Tal Goldfryd, Shiri Gordon, and Tammy Riklin Raviv, "Deep semi-supervised bias field correction of mr images," in *2021 IEEE 18th international symposium on biomedical imaging (ISBI)*. IEEE, 2021, pp. 1836–1840.
- [7] Liangjun Chen, Zhengwang Wu, Dan Hu, Fan Wang, J Keith Smith, Weili Lin, Li Wang, Dinggang Shen, Gang Li, UNC/UMN Baby Connectome Project Consortium, et al., "Abcnet: Adversarial bias correction network for infant brain mr images," *Medical image analysis*, vol. 72, pp. 102133, 2021.
- [8] Attila Simkó, Tommy Löfstedt, Anders Garpebring, Tufve Nyholm, and Joakim Jonsson, "Mri bias field correction with an implicitly trained cnn," in *International Conference on Medical Imaging with Deep Learning*. PMLR, 2022, pp. 1125–1138.
- [9] Chongyi Li, Chunle Guo Guo, and Chen Change Loy, "Learning to enhance low-light image via zero-reference deep curve estimation," in *IEEE Transactions on Pattern Analysis and Machine Intelligence*, 2021.
- [10] Jessica BS Langbaum, Kewei Chen, Wendy Lee, Cole Reschke, Dan Bandy, Adam S Fleisher, Gene E Alexander, Norman L Foster, Michael W Weiner, Robert A Koeppe, et al., "Categorical and correlational analyses of baseline fluorodeoxyglucose positron emission tomography images from the alzheimer's disease neuroimaging initiative (adni)," *Neuroimage*, vol. 45, no. 4, pp. 1107–1116, 2009.
- [11] Nicholas J Tustison, Philip A Cook, Andrew J Holbrook, Hans J Johnson, John Muschelli, Gabriel A Devenyi, Jeffrey T Duda, Sandhitsu R Das, Nicholas C Cullen, Daniel L Gillen, et al., "The antsx ecosystem for quantitative biological and medical imaging," *Scientific reports*, vol. 11, no. 1, pp. 9068, 2021.
- [12] Pamela J LaMontagne, Tammie LS Benzinger, John C Morris, Sarah Keefe, Russ Hornbeck, Chengjie Xiong, Elizabeth Grant, Jason Hassenstab, Krista Moulder, Andrei G Vlassenko, et al., "Oasis-3: longitudinal neuroimaging, clinical, and cognitive dataset for normal aging and alzheimer disease," *medrxiv*, pp. 2019–12, 2019.